







Effect of Deposition Temperature on the Chemical, Structural, Morphology and Electrical Properties of Drop-Cast Graphene Thin Film



Norsakinah Johrin¹, Nur Syafiqah Md Nasir¹, Satri Baco¹, Pak Yan Moh^{1,2}, Jackson H. W. Chang³,
Fuei Pien Chee^{1*}

¹ Faculty of Science and Natural Resources, Universiti Malaysia Sabah, Kota Kinabalu 88400, Malaysia

² Water Research Unit, Faculty of Science and Natural Resources, Universiti Malaysia Sabah, Kota Kinabalu 88400, Malaysia

³ Preparatory Centre for Science and Technology, Universiti Malaysia Sabah, Kota Kinabalu 88400, Malaysia

Corresponding Author Email: fpchee06@ums.edu.my

Copyright: ©2024 The authors. This article is published by IIETA and is licensed under the CC BY 4.0 license (<http://creativecommons.org/licenses/by/4.0/>).

<https://doi.org/10.18280/rcma.340602>

ABSTRACT

Received: 29 August 2024

Revised: 27 September 2024

Accepted: 18 October 2024

Available online: 28 December 2024

Keywords:

graphene oxide (GO), modified Hummers method (MHM), solar cell, energy devices, graphene deposition

Graphene oxide (GO) exhibits excellent electrical, mechanical, thermal, optical properties, and biocompatibility, making it a versatile material with promising applications in various fields. The graphene layers in natural graphite are highly interconnected by pronounced π - π -stacking interactions. Confirmation of successful GO synthesis from graphite flakes using the modified Hummers method (MHM) is achieved through X-ray diffraction (XRD) and Fourier transform and infrared (FTIR) analysis. Subsequently, the GO films were deposited using spin coating and drop casting procedures. The graphene thin films deposited by spin coating exhibit an X-ray diffraction peak at 30.37° , whereas the graphene thin films deposited by drop casting have a peak at 26.63° , indicating successful exfoliation and increased inter-planar spacing in the latter. Graphene thin films deposited via the drop-casting technique undergo three thermal conditions tests incorporating unheated, preheated at 200°C , and post-heated at 80°C . Fourier Transform Infra-Red (FTIR) analysis demonstrates a significant reduction in O-H stretching vibrations after the reaction between GO and annealed temperature at 800°C compared to other thermal conditions. XRD analysis of the preheated at 200°C samples reveals a characteristic peak at 26.635° , indicating successful reduction of GO to graphene. In addition, the analysis shows that graphene particles appear to be separated by a wider distance at room temperature compared to other thermal conditions; with platelet-like crystals visible in the graphite structure on the SEM analysis. The graphene surface displays a linear relationship between current voltage (I-V) across all thermal conditions, highlighting graphene's high conductivity. This analysis suggests that the optimum technique to obtain graphene thin film is by dropping GO onto glass substrates preheated at 200°C . The results indicate a considerable reduction in epoxy and hydroxyl groups, a less pronounced peak in the XRD analysis suggests that the graphite structure is distorted, leading to the successful formation of graphene sheets, and more crumpled thin sheets in the SEM image accumulated to form disordered structure material, respectively.

1. INTRODUCTION

Graphene is a 2D-carbon allotrope with a molecular weight of greater than 106 g/mol and can be regarded both as a solid and a macromolecule. In natural graphite, the graphene layers are strongly bonded by prominent π - π -stacking interactions. There is a non-covalent interlayer bonding between the layers of graphite that contributes significantly to its high thermodynamic stability [1]. In addition, graphene has shown promise in the field of solar cells. Due to the introduction of graphene into the device structure, hybrid organic-inorganic devices have become more efficient [2]. Oxygenated functional groups, including hydroxyl, epoxy, carbonyl, and carboxyl groups, are abundant on the surface of GO. Due to

these properties, GO is a highly hydrophilic material that forms a stable dispersion solution. It can be easily fabricated into graphene-based hybrid composites [3]. Using novel techniques such as photo-thermal or chemical reduction of GO, reduced graphene oxide is used as a stabilizing agent in perovskite cells [4].

Several methods to fabricate graphene include dip coating, chemical vacuum deposition (CVD), spin coating, drop-casting, and many other techniques. First, dip coating is dipping the substrate's material in an aqueous coating, carrying it out, letting it drip dry, and then heating it. The electrochemical impedance and potential dynamic polarisation analyses demonstrated that the graphene dip coatings offered an exceptionally effective protective barrier between the

substrate and the material thin film [5]. However, due to Vander Waals interactions, these sheets have a tendency for experiencing reversible agglomeration and further restack one over the other [6]. Following that, the most preferred technique for producing high-quality, large-area single or few-layer graphene synthesis on metal substrate most notably metal foils right is currently chemical vacuum deposition, or CVD [7]. Graphene films can be produced via standard CVD or PECVD methods on insulator films like sapphire, silicon, and glass without metallic catalysts [8]. However, it needs high temperature in order to process and use expensive catalysts [9, 10]. Next, spin coating enhances graphene dispersion on a substrate and produces a homogeneous nanostructure. Spin-coated thin films and thin film photovoltaic solar cells have demonstrated excellent outcomes using this easy and inexpensive mechanical process [11]. Other than that, simple drop-cast method was used to directly produce graphene oxide sheets with a controlled thickness suspended over an open space [12]. In this context discussed, both spin coating and drop casting are utilized for depositing graphene thin films. Spin coating is an affordable and low-cost method used for fabricating organic solar cell structure. The positive aspects of the drop-casting method, including mechanical characteristics, and electron transparency access for environmental electron microscopy in microfluidic chips or devices with microcracks, warrant further analysis.

The spin coating procedure is a method for forming uniformly thin films of organic compounds on flat substrates that range in thickness from micro to nanometers [13]. During this process, a small amount of liquid coating material is placed at the center of the substrate, which may be stationary or rotating at a low speed. Once the substrate begins to rotate, centrifugal force spreads the coating material evenly across its surface [14]. Using this method, an aqueous solution of graphene oxide (GO) can be uniformly deposited onto an indium tin oxide (ITO) anode. It has been observed that high temperatures (230°C) enhance the conductivity of the GO layer, thereby improving the fill factor (FF) and power conversion efficiency (PCE) of perovskite solar cell (PSC) devices. However, the insulating nature of GO causes its series resistance to increase with thickness, leading to poor performance in PSCs due to thickness-dependent properties [15]. During the rapid spin-coating process, tangential forces cause GO flakes to align toward the wetting surface, depositing them in the wetting region as the solvent evaporates. Consequently, factors such as the wettability of the solution and the concentration of GO influence its distribution on the substrate and the density of GO flakes deposited per unit volume [16].

Another fundamental method is drop casting, which has similar characteristics to dip coating. Regarding the production of GO layers, this is the most basic method [17]. It is necessary to drop GO dispersions on substrates, which are then allowed to dry [18]. By reducing the volume of the GO solution, drop casting can create thinner GO coatings over smaller areas. This cost-effective method enables the integration of graphene and graphene oxide thin films into various electronic and photonic devices, including transparent conductive electrodes, humidity sensors, and optical modulators, through selective area coating [19].

In this study, graphene oxide (GO) is synthesized from graphite using a modified Hummers' method. The research evaluates both spin coating and drop casting techniques for GO deposition while examining the effects of temperature on

graphene thin films. Particular attention is given to the chemical and structural morphology, as well as the current-voltage properties of the films, using drop casting techniques. Since the quality of graphene is significantly influenced by GO as its precursor, the choice of deposition technique is critical in graphene production.

2. EXPERIMENTAL

2.1 Synthesis of graphene oxide

A sample of 1 g graphite flakes and 6 g KMnO_4 is weighed. To prepare a solution with these materials, 120 mL of H_2SO_4 and 13 mL of H_3PO_4 are added to the mixture. The resulting mixture is heated to 50°C for 24 hours. After heating, the mixture is allowed to cool to room temperature. It is then poured into 400 mL of ice containing 8 mL of 30% H_2O_2 , resulting in a graphite oxide suspension. The precipitate is separated by centrifuging the mixture at 4000 rpm for five minutes. The collected precipitate is washed twice with 200 mL of 37 wt% HCl and then washed three times with 200 mL of deionized (DI) water, each wash followed by centrifugation at 4000 rpm for 20 minutes. Once the precipitate is obtained, 400 mL of DI water is added, and the mixture is stirred continuously for 12 hours. To produce a graphene oxide dispersion, the suspension is sonicated for one hour. The suspension is then centrifuged at 4000 rpm for 40 minutes to separate the graphene oxide. The supernatant, a dark-brown mixture containing homogeneously dispersed graphene oxide in water, is collected [3]. Due to the strong interfacial adhesion between the evenly distributed graphene oxide sheets, the samples are freeze-dried under low pressure. During this process, the solvent is sublimated, forming a solid and firm structure [20].

2.2 Deposition of graphene thin film

2.2.1 Deposition of graphene thin film by spin coating

The graphene oxide powder was suspended in water at 15 mg/ml. As shown in Figure 1, the substrate with the graphene oxide solution was allowed to stand for 5s on preheated glass substrates at 200°C. Spin coating was then conducted at 500 rpm for 10 seconds. Following that, the thin films were dried at 80°C in an oven [21].

2.2.2 Deposition of graphene thin film by drop casting

Following the drop-casting technique as shown in Figure 2, the solution was dropped onto glass substrates preheated at 200°C. The substrate with the graphene oxide solution was allowed to stand until dry. After drying, the thin films were annealed at 80°C inside an oven.

2.2.3 Heat treatment on deposition of graphene thin film by drop casting

The drop-casting process will be conducted under 3 different temperature conditions: unheated, preheated at 200°C, and post-heated at 80°C. Initially, the solution is deposited onto glass substrates at room temperature without applying heat, and the drying process is monitored until the graphene oxide layer is fully dry. In the next step, the solution is dropped onto glass substrates preheated to 200°C. Afterward, the graphene thin film is annealed at 80°C in an

oven following air drying on the preheated glass substrate at 200°C, as outlined in the described procedure.

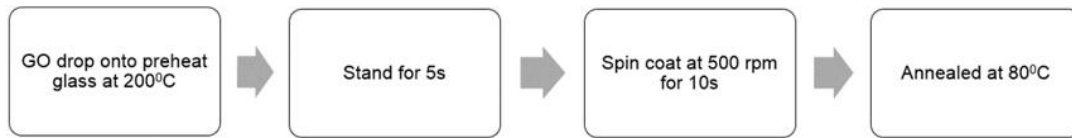


Figure 1. Flowchart illustrating the deposition of graphene thin films using the spin coating method



Figure 2. Flowchart illustrating the deposition of graphene thin films using the drop-casting method

3. RESULTS AND DISCUSSION

3.1 Characterization of synthesized GO

Fourier Transform Infra-Red (FTIR, Perkin Elmer spectrometer) analysis of GO was conducted to determine its structure and functional groups. Figure 3 illustrates the FTIR spectrum of the GO layer. The GO layer vibrational spectrum consists of carbonyl (C = O), aromatic (C = C), carboxyl – (COOH), and hydroxyl (O-H) groups. Observations indicate that a sharp peak at 3343.628 cm^{-1} corresponds to the stretching of carboxyl groups in water molecules adsorbing on GO [22]. GO disperses well in water due to this oxygen-containing functional group [23, 24]. Therefore, it can be concluded that GO is a highly hydrophilic material. It is noted that the peak at 1626.63 cm^{-1} is the result of stretching vibrations of the ketone group (C = O) of carboxylic acid present at the edges of GO and that the graphitic domain of the peak at 1540 cm^{-1} is the result of hybridization with the sp^2 group [25].

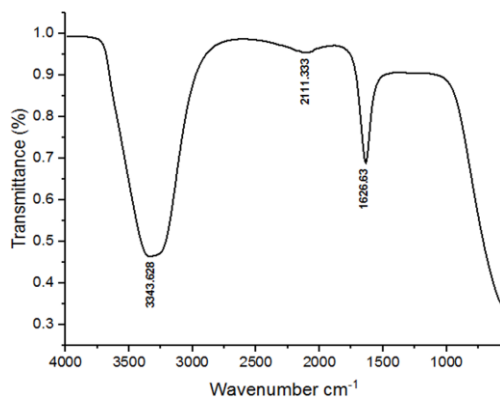


Figure 3. Graph of FTIR spectrum of GO suspension

An X-Ray Diffraction (XRD, Bruker D2 Phaser) analysis was conducted to determine the interlayer changes and crystalline properties of the GO. XRD pattern for GO is shown in Figure 4. A strong diffraction peak for GO was located at $2\theta=10.199^\circ$, comparable to the diffraction peak of GO reference located at $2\theta=10.640^\circ$ [26]. Additionally, a broad diffraction peak was observed at $2\theta=23.628^\circ$ corresponding to an interlayer spacing of about 3.76 Å. The broad interlayer spacing of graphene oxide (GO) is attributed to the presence

of an oxygenated functional group on GO after the intense oxidation treatment of graphite powder and intercalation of water molecules which corresponds to the (002) basal plane with d-spacing 8.48 Å was observed for the GO [23]. These XRD findings provide initial evidence for the formation of graphene oxide (GO) synthesized from Hummer’s method.

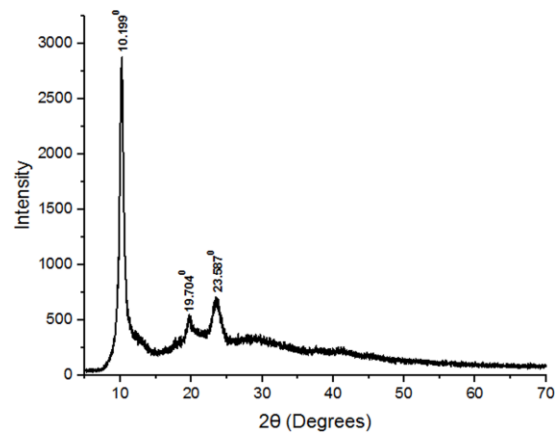


Figure 4. X-ray diffraction spectrum of GO

3.2 Characterization of graphene thin film deposited via spin coating and drop casting techniques

Figure 5 illustrates the measured XRD pattern of graphene thin film deposited using spin coating and drop casting technique respectively. For graphene thin films fabricated by spin coating, the X-ray diffraction peak is observed at 30.37° . There is a shift and increased intensity in the prominent diffraction peak. This indicates a lower oxidation and exfoliation of the sample, maintaining its graphitic structure [27]. Conversely, for graphene thin films deposited by drop casting, the peak is observed at 26.63° . Several literatures reported an X-ray diffraction peak at region $25^\circ\text{-}27^\circ$ for graphene thin films [28]. Based on the observations, the graphene thin film prepared by drop casting closely matches the reports. The interplanar distance between graphene thin films is 3.35 Å, respectively. Graphene thin films produced from graphite powder exhibit an increase in the inter-planar space, indicating successful exfoliation of graphene sheets. The drop-casting technique demonstrates the production of high-quality graphene crystalline thin films [29].

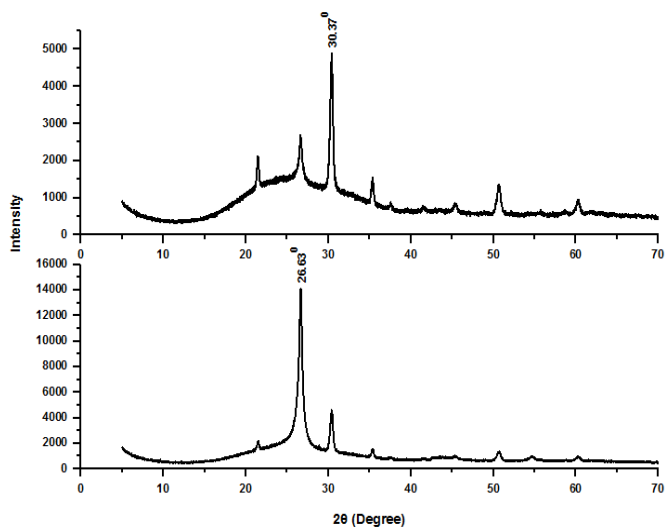


Figure 5. X-ray diffraction spectrum of graphene thin film deposited using (a) Spin-coating and (b) Drop casting

3.3 Characterization of deposition temperature of graphene thin film by drop casting technique

Figure 6(a) Graphene oxide was synthesized by the modified Hummer method (MHM) technique and deposited by drop casting without adding heat under room temperature. Some vibrations point shows its own characteristics and compound.

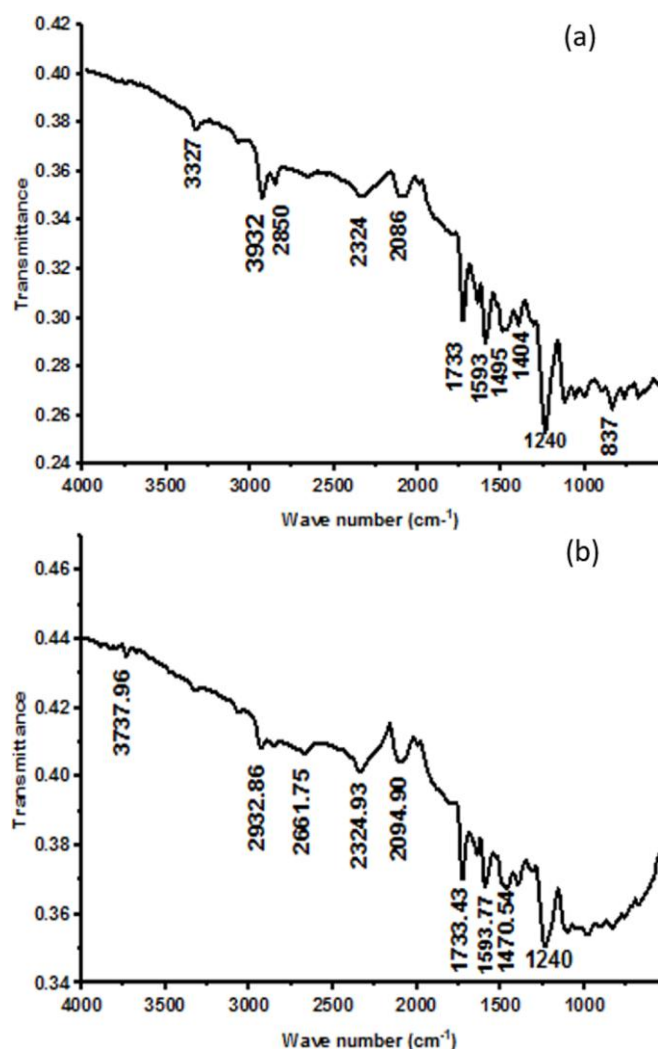


Figure 6. FTIR spectrum of graphene thin film deposited using drop-casting on (a) Unheated, (b) Preheated at 200°C, and (c) Preheated at 200°C and post heated glass at 80°C

For example, GO synthesized from graphite flakes has several oxygen functional groups at 3327 cm^{-1} and 1733 cm^{-1} that refer to the O-H and C-O stretching vibrations. The skeletal vibrations of un-oxidized graphite cause a vibration at 1593 cm^{-1} [30]. The vibrations of 1240 cm^{-1} correspond to the stretching vibrations of O-H, and the vibrations of 837 cm^{-1} correspond to the stretching vibrations of halo compound.

As shown in Figure 6(b), O-H stretching vibrations of GO are reduced from 3327 cm^{-1} to 3737.96 cm^{-1} as a result of the reaction between GO and preheated glass at 200°C. Hybridization with the sp^2 group leads to the graphitic domain of the peak at 1593.77 cm^{-1} . Due to the deoxygenation, epoxy and hydroxyl groups were significantly reduced, while the prominent peak (C-N stretch) was observed at 1470 cm^{-1} [30].

Figure 6(c) shows that O-H stretching vibrations are almost entirely reduced after the reaction between GO and the preheated glass at 200°C and annealed temperature at 80°C. The deoxygenation process caused the epoxy and hydroxyl groups to entirely reduce, which was observed due to the reduction process. The graphitic domain, which is the result of hybridization with the sp^2 group, is not observed in the FTIR spectra for the graphite formation [31].

Based on Figures 6(a)-(c), the difference in the functional group, which is the peak at 1733 cm^{-1} and 1593 cm^{-1} in graphene deposited on the unheated glass, indicates that O-H stretching vibrations of GO are reduced when reacted with the preheated glass at 200°C. Thus, it provides insight into the deduction of the carbonyl group during the reduction process [28].

Figure 7(a) illustrates the measured XRD pattern of graphene oxide deposited onto unheated glass under room temperature using the drop-casting technique. The main diffraction peak at 26.643°. In this case, the as-exfoliated graphene sample is most likely a single-layer or a few layers of graphene sample, since the considerable weakness in intensity may be due to a relatively small amount of material in the multi-layered sheets [32].

As shown in Figure 7(b), the main diffraction peak at 26.635° when graphene oxide reacts with preheated glass at 200°C. According to Barde [33], the shift peaks at 24° to 26°, when graphite oxidation occurs and graphene sheets exfoliate. As graphite oxidizes, d-spacing increases, this can be associated with oxygen-containing functional groups induced by oxides. However, it shows a less intense peak, which

suggests that graphene sheets have formed due to the distorted graphite structure rather than pure graphite diffraction peaks, as reported by Mishra and Ramaprabhu [34].

Figure 7(c) shows that the main diffraction peak at 26.645° . Compared to the graphene oxide drop onto unheated and preheated glass, the main diffraction peak is slightly shifted and more intense due to the less oxidation and exfoliation [27].

Based on the observations as discussed for Figures 7(a)- (c), it is evident that the intensity of the peak is not as pronounced as observed under other thermal conditions, indicating oxidation of graphene after reacting with the preheated glass at 200°C . It suggests that the graphite structure is distorted, leading to the successful formation of graphene sheets.

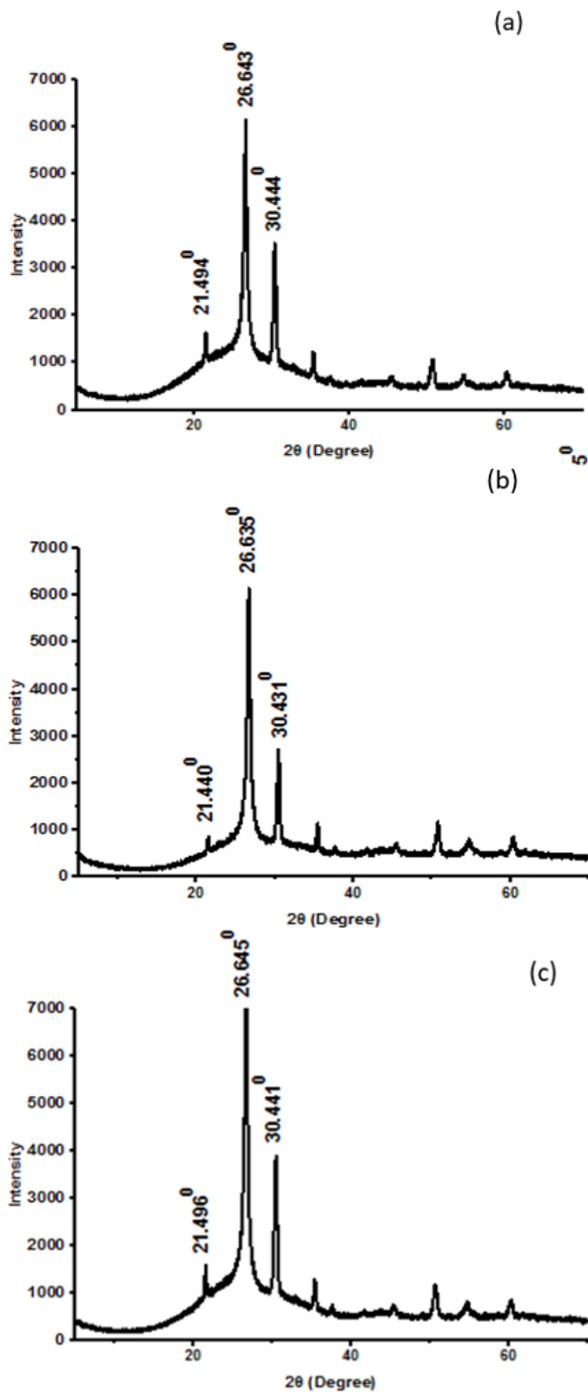


Figure 7. XRD diffraction spectrum of graphene thin film deposited using drop-casting on (a) Unheated (b) Preheated at 200°C (c) Preheated at 200°C and post heated glass at 80°C

Scanning Electron Microscope (SEM S-3400N) was utilized to examine the morphologies of graphene on unheated, preheated and post-heated glass. The micrographs obtained from SEM provided highly magnified image of the surface of a material at x15000 magnification. Figure 8(a) shows the SEM image of the graphene oxide drop-cast on unheated glass. Graphene particles appear to be separated by a wider with a far distance. Furthermore, the wrinkled and layered flakes are visible as reported by Siburian et al. [35].

As shown in Figure 8(b), comparing graphene nanosheets to graphene on non-heated glass, the graphene nanosheets have a wrinkled surface, smaller pores, and uniform sizes. To form an irregular solid, these nano sheets aggregate with a thin layer randomly [35]. In the reaction between graphene and preheated glass, crumpled thin sheets accumulated to form disordered structure material [36].

Figure 8(c) shows the SEM image of graphene on preheated at 200°C and post-heated glass at 80°C . As can be seen, graphite has a layered structure due to the presence of many stacks [35, 37]. According to Hidayah et al., platelet-like crystals were visible in the graphite structure [27].

Based on Figures 8(a)-(c), in comparison to other temperature conditions, graphene reacted with preheated glass at 200°C , exhibiting smaller, thinner forms and aggregation while indicating a smoother accumulation. However, the exfoliation process of the structure reduces visibility.

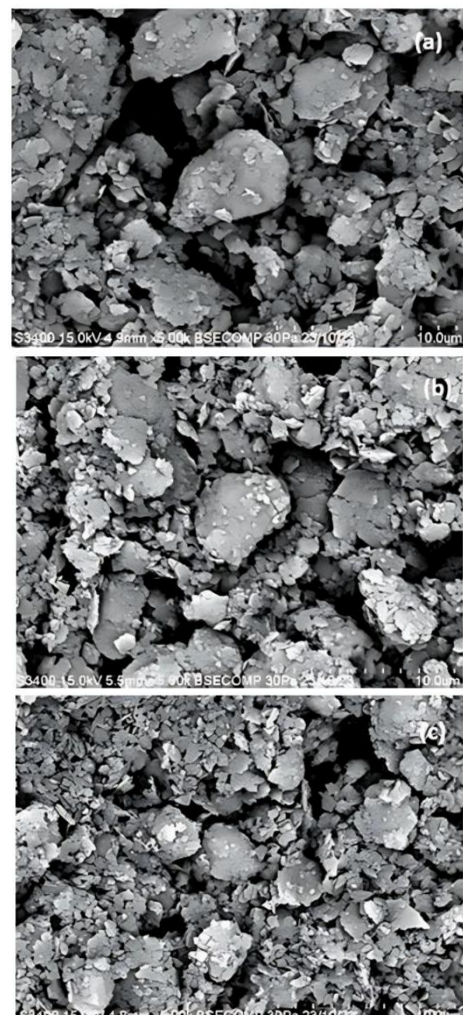


Figure 8. SEM image of graphene thin film deposited using drop-casting on (a) Unheated (b) Preheated at 200°C , and (c) Preheated at 200°C and post heated glass at 80°C

Based on the Figure 9 current-voltage (I-V Keithley 24000) curves, no significant changes are observed even though there is an influence of heat with the graphene during deposition. Notably, the graphene surface demonstrates a linear current-voltage relationship [36], which implies that electrons migrate very effectively and have excellent mobility on the graphene layer [38]. The linear relationship between applied current and voltage closely follows Ohm's law suggesting the absence of heat-induced flaws in the graphene lattices. This behaviour is consistent with graphene's inherent high conductivity material.

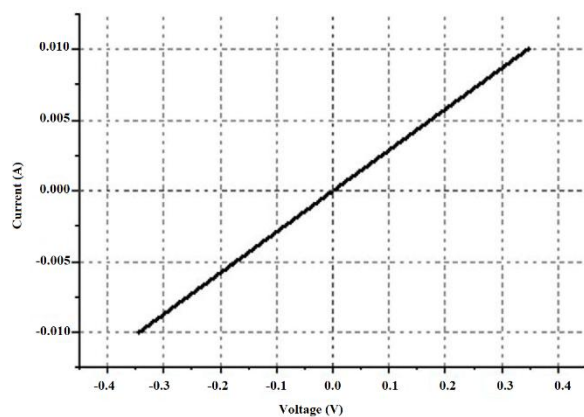


Figure 9. Current-Voltage (I-V) of graphene thin film deposited using drop-casting under three different heat treatment

4. CONCLUSION

In conclusion, GO were successfully prepared by using modified Hummers method (MHM) synthesis. This research used XRD, FTIR, SEM, and I-V analysis to characterize graphene thin films. The comparison result of XRD shows the graphene thin films deposited by drop casting have a peak at 26.63°, indicating successful exfoliation and increased interplanar spacing in the latter. Graphene thin films formed via the drop-casting technique undergo three thermal conditions tests: unheated, preheated at 200°C, and post-heated glass at 80°C. Besides, FTIR spectrum shows that GO decreases its O-H stretching vibrations and has graphitic domains result from the hybridization of the sp² group when reacted with preheated glass at 200°C. Using X-ray diffraction (XRD), samples preheated at 200°C show a distinctive peak at 26.635°. The results show that graphite was successfully oxidized into GO, whereas graphene was reduced from GO. Additionally, graphene particles appear to be separated by a wider distance when no heat is applied under room temperature, compared to preheated at 200°C and post-heated glass at 80°C. The presence of multiple stacks also contributes to the layered structure of graphite. The graphene surface shows a linear current-voltage (I-V), given that graphene is very conductive. The optimal thermal conditions can be achieved by dropping graphene oxide (GO) onto glasses at 200°C. This will result in significantly reduced epoxy and hydroxyl groups, a less prominent peak in the XRD analysis indicating that the distorted graphite structure rather than pure graphite diffraction peaks, and a SEM image with more wrinkled surface, smaller pores, and uniform sizes. The ability to create high-quality graphene thin films is the reason that makes findings in graphene deposition techniques significant. Realizing graphene's potential in materials science, and next-

generation electronics depends on these achievements. For high-performance applications, precise control over material properties will be made possible by further research on rGO deposition processes, with an emphasis on scalability, film quality, and uniformity improvements.

ACKNOWLEDGEMENTS

The authors would like to extend their gratitude to Malaysian Ministry of Higher Education for their support in conducting this research under the Fundamental Research Grand Scheme (FRGS) Year 2022, FRGS/1/2022/STG07/UMS/02/01 and UMSGreat, Year 2023, GUG0579-1/2023.

REFERENCES

- [1] Eigler, S., Hirsch, A. (2014). Chemistry with graphene and graphene oxide—challenges for synthetic chemists. *Angewandte Chemie International Edition*, 53(30): 7720-7738. <https://doi.org/10.1002/anie.201402780>
- [2] Tyagi, S., Singh, P.K., Tiwari, A.K. (2022). Photovoltaic parameter extraction and optimisation of ZnO/GO based hybrid solar trigeneration system using SCAPS 1D. *Energy for Sustainable Development*, 70: 205-224. <https://doi.org/10.1016/j.esd.2022.08.001>
- [3] Nguang, S.Y., Liew, A.S.Y., Chin, W.C., Tahir, N., Arshad, S.E., Chee, F.P., Moh, P.Y. (2022). Effect of graphene oxide on the energy level alignment and photocatalytic performance of Engelhard Titanosilicate-10. *Materials Chemistry and Physics*, 275: 125198. <https://doi.org/10.1016/j.matchemphys.2021.125198>
- [4] Kang, A.K., Zandi, M.H., Gorji, N.E. (2019). Simulation analysis of graphene contacted perovskite solar cells using SCAPS-1D. *Optical and Quantum Electronics*, 51: 1-9. <https://doi.org/10.1007/S11082-019-1802-3>
- [5] Chong, W.S., Gan, S.X., Al-Tuwir, H.M., Chong, W.Y., Lim, C.S., Ahmad, H. (2020). Nanolitre solution drop-casting for selective area graphene oxide coating on planar surfaces. *Materials Chemistry and Physics*, 249: 122970. <https://doi.org/10.1016/j.matchemphys.2020.122970>
- [6] Sahai, R.S.N., Jadhav, P.K., Solanke, S., Gawande, S.H. (2024). Sustainable machining of EN19 steel: Efficacy of eco-friendly cooling fluids and hybrid optimization techniques. *Precision Mechanics & Digital Fabrication*, 1(1): 41-54. <https://doi.org/10.56578/pmdf010105>
- [7] Naghdi, S., Rhee, K.Y., Kim, M.T., Jaleh, B., Park, S.J. (2016). Atmospheric chemical vapor deposition of graphene on molybdenum foil at different growth temperatures. *Carbon Letters*, 18: 37-42. <https://doi.org/10.5714/CL.2016.18.037>
- [8] Xu, S., Zhang, L., Wang, B., Ruoff, R.S. (2021). Chemical vapor deposition of graphene on thin-metal films. *Cell Reports Physical Science*, 2(3): 100372. <https://doi.org/10.1016/j.xcrp.2021.100372>
- [9] Khodabakhshi, S., Kiani, S., Niu, Y., White, A.O., et al. (2021). Facile and environmentally friendly synthesis of ultramicroporous carbon spheres: A significant improvement in CVD method. *Carbon*, 171: 426-436. <https://doi.org/10.1016/j.carbon.2020.08.056>
- [10] Tewari, A., Gandla, S., Bohm, S., McNeill, C.R., Gupta,

- D. (2019). Remarkable wettability of highly dispersive rGO ink on multiple substrates independent of deposition techniques. *FlatChem*, 16: 100110. <https://doi.org/10.1016/j.flatc.2019.100110>
- [11] Zabihi, F., Chen, Q., Xie, Y., Eslamian, M. (2016). Fabrication of efficient graphene-doped polymer/fullerene bilayer organic solar cells in air using spin coating followed by ultrasonic vibration post treatment. *Superlattices and Microstructures*, 100: 1177-1192. <https://doi.org/10.1016/j.spmi.2016.10.087>
- [12] Krueger, M., Berg, S., Stone, D.A., Strelcov, E., et al. (2011). Drop-casted self-assembling graphene oxide membranes for scanning electron microscopy on wet and dense gaseous samples. *ACS Nano*, 5(12): 10047-10054. <https://doi.org/10.1021/nn204287g>
- [13] Miandal, K., Tak, H.H., Mohamad, K.A., Chee, F.P., Alias, A. (2017). The structural and optical properties of poly (Triarylamine)(PTAA) thin films prepared at different spin rate using spin coating method. *Advanced Science Letters*, 23(2): 1337-1339. <https://doi.org/10.1166/asl.2017.8363>
- [14] Mustafa, H.A.M., Jameel, D.A. (2021). Modeling and the main stages of spin coating process: A review. *Journal of Applied Science and Technology Trends*, 2(2): 119-123. <https://doi.org/10.38094/jastt203109>
- [15] Liu, J., Durstock, M., Dai, L. (2014). Graphene oxide derivatives as hole-and electron-extraction layers for high-performance polymer solar cells. *Energy & Environmental Science*, 7(4): 1297-1306. <https://doi.org/10.1039/c3ee42963f>
- [16] Guo, Y., Di, C. A., Liu, H., Zheng, J., Zhang, L., Yu, G., Liu, Y. (2010). General route toward patterning of graphene oxide by a combination of wettability modulation and spin-coating. *ACS Nano*, 4(10): 5749-5754. <https://doi.org/10.1021/nn101463j>
- [17] Kwon, O., Choi, Y., Choi, E., Kim, M., Woo, Y.C., Kim, D.W. (2021). Fabrication techniques for graphene oxide-based molecular separation membranes: Towards industrial application. *Nanomaterials*, 11(3): 757. <https://doi.org/10.3390/nano11030757>
- [18] Kumar, A.K.S., Zhang, Y., Li, D., Compton, R.G. (2020). A mini-review: How reliable is the drop casting technique?. *Electrochemistry Communications*, 121: 106867. <https://doi.org/10.1016/j.elecom.2020.106867>
- [19] Liu, J., Hua, L., Li, S., Yu, M. (2015). Graphene dip coatings: An effective anticorrosion barrier on aluminum. *Applied Surface Science*, 327: 241-245. <https://doi.org/10.1016/j.apsusc.2014.11.187>
- [20] Valencia, C., Valencia, C.H., Zuluaga, F., Valencia, M.E., Mina, J.H., Grande-Tovar, C.D. (2018). Synthesis and application of scaffolds of chitosan-graphene oxide by the freeze-drying method for tissue regeneration. *Molecules*, 23(10): 2651. <https://doi.org/10.3390/molecules23102651>
- [21] Kymakis, E., Stratakis, E., Stylianakis, M. M., Koudoumas, E., Fotakis, C. (2011). Spin coated graphene films as the transparent electrode in organic photovoltaic devices. *Thin Solid Films*, 520(4): 1238-1241. <https://doi.org/10.1016/j.tsf.2011.04.208>
- [22] He, D., Peng, Z., Gong, W., Luo, Y., Zhao, P., Kong, L. (2015). Mechanism of a green graphene oxide reduction with reusable potassium carbonate. *RSC Advances*, 5(16): 11966-11972. <https://doi.org/10.1039/c4ra14511a>
- [23] Chen, J., Yao, B., Li, C., Shi, G. (2013). An improved Hummers method for eco-friendly synthesis of graphene oxide. *Carbon*, 64: 225-229. <https://doi.org/10.1016/j.carbon.2013.07.055>
- [24] Hanifah, M.F.R., Jaafar, J., Aziz, M., Ismail, A.F., Rahman, M.A., Othman, M.H.D. (2015). Synthesis of graphene oxide nanosheets via modified Hummers' method and its physicochemical properties. *Jurnal Teknologi*, 74(1): 195-198. <https://doi.org/10.11113/jt.v74.3555>
- [25] Shahriary, L., Athawale, A.A. (2014). Graphene oxide synthesized by using modified hummers approach. *International Journal of Renewable Energy and Environmental Engineering*, 2(1): 58-63.
- [26] Surekha, G., Krishnaiah, K.V., Ravi, N., Suvarna, R.P. (2020). FTIR, Raman and XRD analysis of graphene oxide films prepared by modified Hummers method. *Journal of Physics: Conference Series*, 1495: 012012. <https://doi.org/10.1088/1742-6596/1495/1/012012>
- [27] Hidayah, N.M.S., Liu, W.W., Lai, C.W., Noriman, N.Z., Khe, C.S., Hashim, U., Lee, H.C. (2017). Comparison on graphite, graphene oxide and reduced graphene oxide: Synthesis and characterization. *AIP Conference Proceedings*, 1892(1): 150002. <https://doi.org/10.1063/1.5005764>
- [28] Aziz, M., Halim, F.S.A., Jaafar, J. (2014). Preparation and characterization of graphene membrane electrode assembly. *Jurnal Teknologi*, 69(9): 11-14. <https://doi.org/10.11113/jt.v69.3388>
- [29] Vasanthi, V., Gayathri, S., Anitha, K., Ramakrishnan, V. (2017). Exfoliation of high-quality graphene in volatile and nonvolatile solvents. *Graphene Technology*, 2: 29-40. <https://doi.org/10.1007/s41127-017-0006-5>
- [30] Sudhakar, S., Jaiswal, K.K., Peera, S.G., Ramaswamy, A.P. (2017). Green synthesis of N-graphene by hydrothermal-microwave irradiation for alkaline fuel cell application. *International Journal of Recent Scientific Research*, 8(8): 19049-19053. <https://doi.org/10.24327/ijrsr.2017.0808.0619>
- [31] Bag, S., Raj, C.R. (2016). On the electrocatalytic activity of nitrogen-doped reduced graphene Oxide: Does the nature of nitrogen really control the activity towards oxygen reduction?. *Journal of Chemical Sciences*, 128: 339-347. <https://doi.org/10.1007/s12039-016-1034-z>
- [32] Wang, W., Wang, Y., Gao, Y., Zhao, Y. (2014). Control of number of graphene layers using ultrasound in supercritical CO₂ and their application in lithium-ion batteries. *The Journal of Supercritical Fluids*, 85: 95-101. <https://doi.org/10.1016/j.supflu.2013.11.005>
- [33] Barde, W.S. (2020). Synthesis of Graphene Oxide (GO) and Reduced Graphene Oxide (RGO): its Characterization by XRD, UV-VIS Spectroscopy and measurement of DC conductivity. *Journal of Emerging Technologies and Innovative Research*, 7(2): 287-291.
- [34] Mishra, A.K., Ramaprabhu, S. (2011). Functionalized graphene sheets for arsenic removal and desalination of sea water. *Desalination*, 282: 39-45. <https://doi.org/10.1016/j.desal.2011.01.038>
- [35] Siburian, R., Sihotang, H., Lumban Raja, S., Supeno, M., Simanjuntak, C. (2018). New route to synthesize of graphene nano sheets. *Oriental Journal of Chemistry*, 34(1): 182-187. <https://doi.org/10.13005/ojc/340120>
- [36] Zhang, J., Zhao, C., Hu, P.A., Fu, Y.Q., et al. (2013). A UV light enhanced TiO₂/graphene device for oxygen sensing at room temperature. *RSC advances*, 3(44):

22185-22190. <https://doi.org/10.1039/c3ra43480j>
[37] Zhang, C.J., Xu, L.G., Liu, P.S. (2024). Formulation of stiffness and strength characteristics of flexible wire ropes and their application in photovoltaic support structures. *Precision Mechanics & Digital Fabrication*, 1(2): 66-74. <https://doi.org/10.56578/pmdf010202>

[38] Johrin, N., Chee, F.P., Nasir, S., Moh, P.Y. (2023). Numerical study and optimization of GO/ZnO based perovskite solar cell using SCAPS. *AIMS Energy*, 11(4): 683-693. <https://doi.org/10.3934/energy.2023034>